Biointerface Research in Applied Chemistry
Platinum Open Access Journal (ISSN: 2069-5837)

Article
Volume 11, Issue 1, 2021, 7847 - 7859
https://doi.org/10.33263/BRIAC111.78477859

Molecular Modeling Analyses for Modified Biopolymers

Amina Omar [1], Hend Ezzat [2], Hanan Elhaes [3], Medhat A. Ibrahim [4]

[1] Physics Department, Biophysics Branch, Faculty of Science, Ain Shams University, 11566 Cairo, Egypt
[2] Nano Technology Unit, Space lab, Solar and Space Research Department, National Research Institute of Astronomy and Geophysics (Nano NRIAG), 11421 Helwan, Cairo, Egypt
[3] Physics Department, Faculty of Women for Arts, Science and Education, Ain Shams University, 11757 Cairo, Egypt
[4] Molecular Spectroscopy and Modeling Unit, Spectroscopy Department, National Research Centre, 33 El-Bohouth St., 12622 Dokki, Giza, Egypt
* Correspondence: medahmed6@yahoo.com;

Scopus Author ID 8641587100
Received: 31.05.2020; Revised: 26.06.2020; Accepted: 28.06.2020; Published: 4.07.2020

Abstract: Biopolymer blends and structural modifications with phenol and hydroxymethylcarbonyl (HMC) are studied to show the ability to interact with amino acids as promising to act as HIV protease inhibitors. Chitosan (Cs), cellulose (Cel), starch (Str) and gelatin (Gel) as well as their blends as Cs/Cel; Cs/Str; Cs/Gel with ratios 3:1; 2:2; 1:3 were subjected to molecular modeling. These biopolymers, as well as their blends, are calculated with quantum mechanical calculations at PM6 level of theory. QSAR, surface area, and volume properties of the interaction of phenol and HMC upon Cs/Cel; Cs/Str; Cs/Gel in the different positions of the four units are calculated at the same level of theory. QSAR descriptors for studied polymers show a change in their physical properties as result of blending. Depending on QSAR calculations, the interaction of phenol and HMC with Cs/Cel and Cs/Str blends for ratio 1:3 through the first unit increases the reactivity of these modified structures. The solubility of modified blends is increased by increasing chitosan units in the proposed modified blends. The surface area of modified Cs/Cel ratios increases comparing with modified Cs/Str and Cs/Gel ratios. This recommends the modified blends of Cs/Cel ratio can be used as promising HIV protease inhibitors drugs.

Keywords: Biopolymer; PM6; QSAR; Chitosan; Nanocomposite.

1. Introduction

Polymers, as well as their blends incorporated with various nanoparticles, had been fabricated for effective use in enhanced magnetic, photocatalytic, hydrogen extraction, electrode material, and to improve the bioactivity. With different processing and functionalization, polymers could produce cost-effective materials for different applications [1-3]. Electrospinning is a promising technique that fabricates nanofibers and could tailor both synthetic and biopolymers for different applications [4]. Simultaneous functionalization and/or post-modification of as-spun nanofibers with biomolecules have been explored in order to serve the distinct objectives set out in the aforementioned field [5]. Another biopolymer such as cellulose acetate (CA) was fabricated into nanofibers, which served the purpose in the sustained delivery of expensive drugs, holding a minute payload of drugs with fewer side effects [6]. One of the interesting chemical modifications; includes exploiting glutaraldehyde as a crosslinking agent and/or by exploiting sol-gel coating of decyltrimethoxysilane and tetraethyl orthosilicate to block the hydrophilic sites in the CA chains [7]. Chitosan, one of the

polysaccharide family, own unique hydrogen bonding, dedicates it for many applications. Many researchers reported the biological applications of chitosan according to its biodegradable nature. Many research papers are interested in the production of chitosan and its various applications in different fields. Chitosan is a potential biopolymer in food processing applications, drug delivery systems formulations, and industrial and energy production processes [8-10]. Developments in the biomaterial research are now widely used to fabricate *in vitro* platforms for differentiation of progenitor cell population as well as implantable tissue engineering scaffolds [11]. Another application related to this topic is in cardiac heart treatment, which is very important, especially for making new tissue for muscle treatment. Cardiac cell therapy is very important for improving heart function and especially of the permanent failure of muscle functions. Embedding cells into 3D biodegradable scaffolds may better preserve cell survival and enhance cell engraftment after transplantation, consequently improving cardiac cell therapy compared with direct intramyocardial injection of isolated cells [12]. Nowadays, it is well known that the disease which is affecting the cornea of the human eye is the main reason for blindness all over the world [13]. Chitosan and other biopolymers may be enhanced by the introduction of a small amount of nanoscale materials in the form of nanometal oxide. Furthermore, Cs has been reported to disperse and stabilize several nanoparticles to produce more potent antimicrobial nanocomposites [14-15]. Chitosan-based nanocomposites show potential applications in the field of wastewater treatment based upon its potential antimicrobial benefits [16]. However, to avoid environmental hazardous exists for Cs nanocomposites according to nanomaterial toxicity in-vitro and in-vivo, it is important to evaluate the biological effects of nanoparticles [17-18]. The aquatic environmental risk assessment for chitosan/silver, copper, and carbon nanotube were studied [19]. Loading Cs matrix with nanoparticles improves the potency of their antimicrobial properties. Multi-wall carbon nanotubes with chitosan have been investigated for the removal of picric acid from aqueous solutions. Different factors affecting the sorption process were studied [20]. Results indicated that picric acid could be desorbed up to 90% at pH = 9. The chitosan nanocomposite could be reutilized up to the 5th cycle of regeneration.Chitosan-TiO_2 nanocomposite was prepared for the selective and quantitative removal of Rose Bengal dye from industrial wastewater [21]. The prepared composite indicated high performance according to its high surface area (95.38m2/g) with relatively uniform mesoporous channels that allowed an exceptional uptake of the dye (qm = 79.365 mg/g) and reflected the high selectivity of the composite as compared with pure Cs. The unique properties of Cs dedicate it for many applications rather than medical such as environmental applications [22-29]. Experimental synthesis of bioactive compounds consumes both time and money. Modeling rationalizes the synthesis, and then drastically reduces the time and the cost. One of the leading computational routes in this field is the Quantitative Structure-Activity Relationship, which is termed (QSAR). QSAR could solve the major problems of designing bioactive compounds such as drugs. QSAR could be defined as a tool that quantifies the relationship between the physicochemical properties of the compound with its biological activity. Thus this produces a mathematical model that guides us as to how the structural or physicochemical properties of the molecules should be changed. The assessment of the compound activity is described throughout some calculated parameters called descriptors [30-34]. QSAR for drug design requires to know the conformational properties of the molecules in liquids and the orientation with the receptor for the interaction. This is called molecular recognition for molecular systems. For a given interaction between two molecules, there are repulsion and attractions; one

molecule act as ligand while the other act as a receptor [35]. The key factor in this interaction is the free energy, which is impacted by the change in degrees of freedom of both molecules. It is stated that the traditional 2D-QSAR routes have been established for predicting the reaction rate constants [36]. It exhibits good performances for the degradation behaviors of chemical, biological compounds [37]. Another class of QSAR is now known as 3D-QSAR, in which it is developed to study the relationships between biological/chemical behaviors and the structural parameters [38]. The most representative 3D-QSAR models are the comparative molecular field analyses and the comparative molecular similarity index analysis. There is another class of QSAR is developed recently termed 4D-QSAR this route of QSAR is serving to find the receptor binding site through conformers of various chemical structures with the same active properties [39-41]. In this work PM6 molecular modeling used to study QSAR, surface area, and volume properties of the interaction of phenol and HMC upon Cs/Cel; Cs/Str; Cs/Gel in the different positions. Such studies are applied to show the ability of that blends to intact with amino acids as promising to act as HIV protease inhibitors.

2. Materials and Methods

2.1. Calculations details.

The calculations of Cs, Cel, Str, and Gel as well as their blends as Cs/Cel; Cs/Str; Cs/Gel were carried using SCIGRESS program soft code at Spectroscopy Department, National Research Centre, Cairo, Egypt [42]. First, the structure is optimized to locate the energy minimum then QSAR, surface area, and volume properties of the interaction of phenol and HMC upon Cs/Cel; Cs/Str; Cs/Gel in the different positions for the studied structure were calculated at PM6 semiempirical quantum mechanical method.

3. Results and Discussion

3.1. Building the model molecules.

Four biopolymers were chosen, namely Cs, Cel, Str, and Gel. These suggested models consist of four subunits for each biopolymer. Blending between the studied biopolymers were tried as Cs/Cel; Cs/Str; Cs/Gel. The blending ratios were tried as respective rations 3:1; 2:2; 1:3 for each structure in these ratios. For each structure of biopolymers and its blends, phenol and HMC are added to the four different subunits in each structure. Figures 1, 2, and 3 show an example of optimized investigated compounds of Cs, Str, and Gel, respectively, interact with phenol and HMC. The compound in figure 1 is consists of Cs four subunits interacted through NH position of the first subunit with phenol and HMC. For Cs subunit, the phenol and HMC tried to interact through the NH position of the subunit according to our previous work [43]. While the compound in figure 2 of Str interact through OH position of first subunit. For Gel in figure 3, phenol and HMC is interacted through OH or NH.

3.2. QSAR Calculation.

The models' molecules of the interaction of phenol and HMC upon Cs/Cel different ratios in the different positions of the four units are shown in figure 4. Some calculated QSAR properties of the interactions of phenol and HMC upon Cs/Cel different ratios in the different positions of the four units are listed in table 1. These QSAR parameters are log P, dipole moment, total energy, total frontier molecular orbital energy gap ΔE (calculated as LUMO–

HOMO energy difference), polarizability, heat of formation, ionization potential, surface area, and volume.

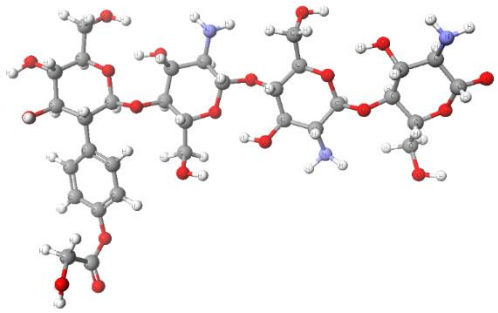

Figure 1. An example of optimized an investigated compound of chitosan interacts with phenol and hydroxymethylcarbonyl (HMC) through NH calculated at PM6.

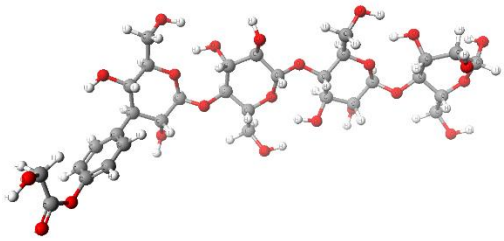

Figure 2. An example of optimized an investigated compound of starch interacts with phenol and hydroxymethylcarbonyl (HMC) through OH calculated at PM6.

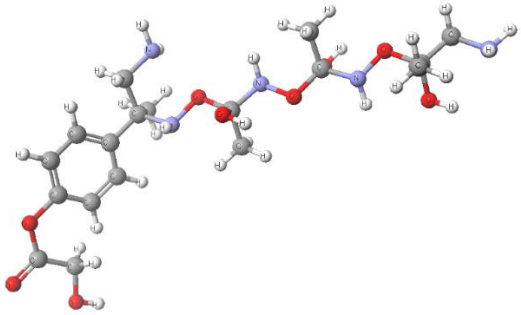

Figure 3. An example of optimized an investigated compound of gelatin interacts with phenol and hydroxymethylcarbonyl (HMC) through OH calculated at PM6.

Log P indicates whether the compound is hydrophilic or hydrophobic. If log P gives a high value or positive value, the molecule will be hydrophobic while log P gives a lower value or negative value, the molecule will be hydrophilic. From table 1, which shows the different ratios of Cs/Cel blend interacted with phenol and HMC through four subunits for every Cs/Cel ratio. With increasing the ratio of Cel to Cs, the hydrophobicity increase due to decreases of amino group NH_2 of rough four Cs subunit. So, the compounds of Cs interact with phenol and HMC through four subunits (Cs4-Cs1, Cs4-Cs2, Cs4-Cs3, and Cs4-Cs4) show a lower value -5.27 comparing with the other compounds with the higher ratio of Cel. By increasing Cel ratio as Cs/Cel ratio 3:1, the hydrophilicity increase (-4.92) due to also interacting of phenol and HMC with Cs subunits in these compound (Cs3:Cel1-Cs1, Cs3:Cel1-Cs2 and Cs3:Cel1-Cs3) while this value is decreased again when phenol and HMC interact through Cel subunit (Cs1:Cel1-Cel4) and become -5.36. The same behavior is happened to the other compounds with increasing the ratio of Cel until reach to Cel compound of the log P value is - 4.32.

Figure 5 and figure 6 show the interaction of phenol and HMC with Cs/Str and Cs/Gel ratios, respectively, at the different four units position.

The same behaviors have happened for Cs/Str, and Cs/Gel different ratios interact with phenol and HMC through four subunits of these ratios, as shown in table 2 and table 3. For Cs/Str, the value of log P increases with an increased ratio of Str. It is - 4.92 for 3:1 ratio until it reaches to -4.32 for the Str only without Cs. There is an increase of hydrophilicity of some compounds as Cs3:Str1-St4, which interacts with phenol and HMC through Str fourth subunit (-6.45). For Cs/Gel ratios, the hydrophobicity increases more with increase ratio of Gel to Cs comparing with other ratios of Cs/Cel and Cs/Str. Total energy for Cs/Cel and Cs/Str interacted with phenol, and HMC is slightly the same. It changed from -305446 Kcal/mol for Cs4-Cs3 to -310672Kcal/mol for Cel4-Cel4. These mean the increasing stability by increasing the ratio between Cs/Cel and Cs/Str compounds. For Cs/Gel compounds, the stability decrease with increasing Cs/Gel ratios. The reactivity of suggested compounds is calculated by the three parameters dipole moments, ΔE and ionization potential. The dipole moments are changed for different ratios of Cs/Cel, Cs/Str, and Cs/Gel modified by phenol and HMC in every subunit in these ratios. If the value of dipole moment increases, then it is reactivity increases, which indicates the more interactions of these compounds with other systems [44]. For Cs/Cel in table 1 show, the dipole moment of the compound with four Cs subunits modified with phenol and HMC through the second Cs unit (Cs4-Cs2) is 6.23 which is showing a higher reactivity comparing with other compounds in the same ratio. The increasing ratio of Cel to Cs increases the reactivity and dipole moment of compounds until reach to Cel 4 subunits modified with phenol and HMC through Cel third subunit (Cel4-Cel3) which is equal to 8.10. For the frontier molecular orbital energy gap (ΔE), the smaller of its value, the more reactive of this compound with its surrounding. According to table 1, the compounds Cs4-Cs2, Cs3:Cel1-Cel4, Cs2-Cel2-Cel4, and Cel4-Cel3 have a lower ΔE value comparing with the other compounds in the different ratios. This indicates that these compounds are more reactive with the surrounding system. The ionization potential (i.e., the electron detachment energy) is the energy necessary to eliminate an electron from the molecule to a practically infinite distance [45]. The ionization potential decreases with increasing the ratios of Cs/Cel ratios. This means that the compounds with lower ionization potential can easily remove an electron, comparing with other compounds which can hardly remove an electron and interact with other systems. For Cs based compounds, the more reactive compound is Cs4-Cs2, which is modified with phenol and MCH through the second Cs subunit. Due to its higher dipole moment (6.225), lower ΔE (9.018 eV), and ionization potential (-9.858 eV). By increasing ratios of Cs/Cel as 3:1 (Cs3:Cel1-Cel4), 2:2 (Cs2:Cel2-Cel3) and 1:3 (Cs1:Cel3-Cel2) are the more reactive compounds. For Cel based compounds, the more reactive compound is Cel4-Cel3, which is modified with phenol and HMC through the third Cel subunit. For Cs/Str compounds (table 2), the reactivity increases with increases in Cs/Str ratios. The compounds Cs3:Str1-Cs1, Cs2:Str2-Cs2 and Cs1:Str3-Cs1 show a more reactive compounds in Cs/Str ratios because of a higher dipole moment (9.74, 6.14 and 10.15respectively), lower ΔE (8.98 eV, 9.17 eV and 9.15 eV respectively) and lower ionization potential (-10.02 eV, -10.16 eV and -10.29 eV respectively). For Str based compounds, the compound Str4-Str1which modified through first Str subunit is more reactive. For Cs/Gel ratios (table 3), the compounds Cs3:Gel1-Cs2, Cs2:Gel2-Gel4, and Cs1:Gel3-Gel4 is more reactive with increasing ratios of Cs/Gel ratios.

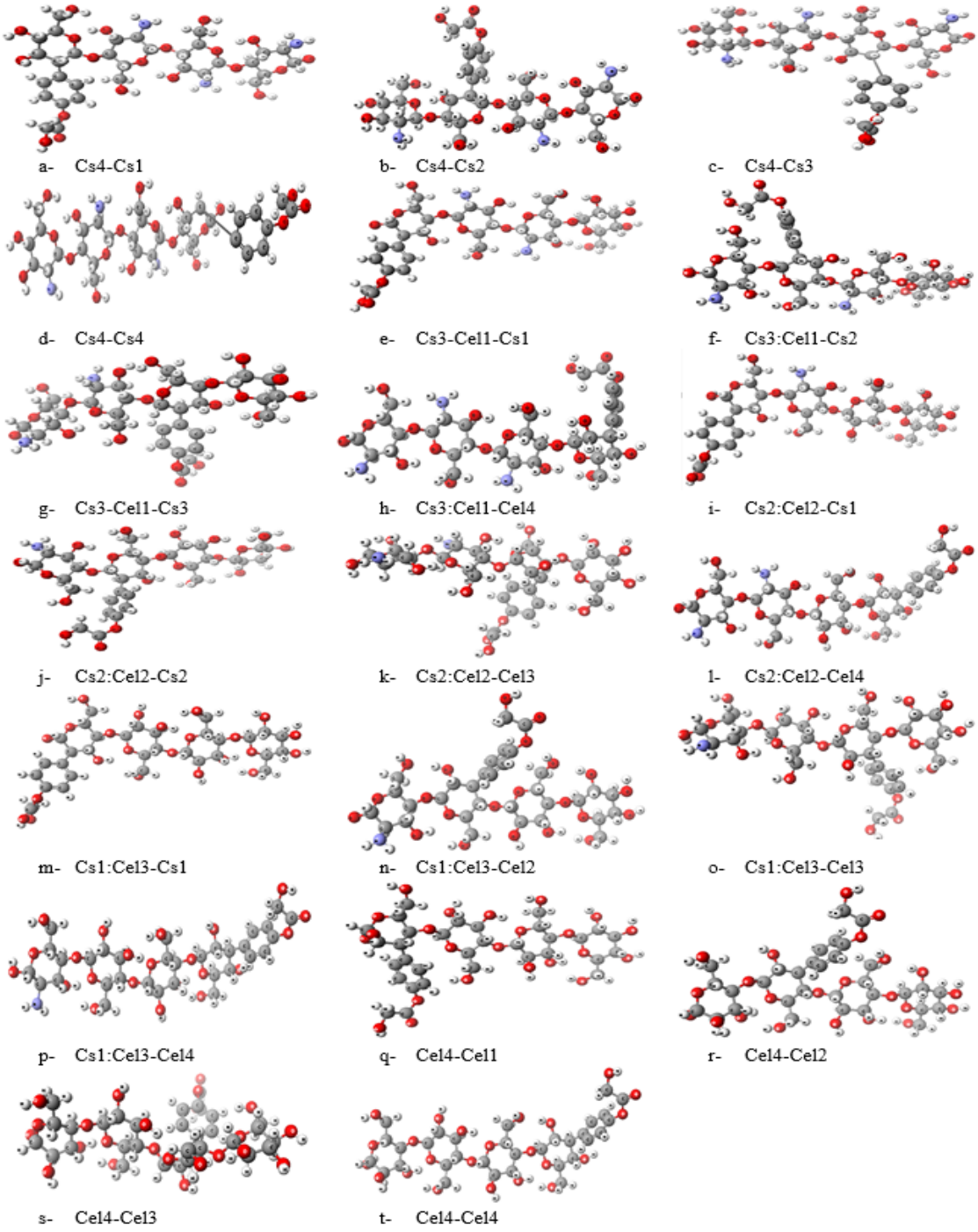

Figure 4. Optimized structure of chitosan/cellulose ratios with interaction phenol and hydroxymethylcarbonyl for different four units position calculated at PM6 level of theory.

For Gel-based compound, the more reactive compounds are Gel compound interact through OH of forth Gel subunit (Gel4-Gel4) the dipole moment is 9.08, ΔE (8.84 eV) and ionization potential (-9.39 eV) and Gel compound interact through NH of forth gelatin subunit (Gel4-Gel4 NH) the dipole moment is 7.37, ΔE (9.09 eV) and ionization potential (-9.59 eV). The next QSAR parameter is the heat of formation. The heat of formation is known as the change in enthalpy accompanying the formation of one mole of a compound from its elements in their natural and stable states, under standard conditions of one atmosphere at a given temperature [46].

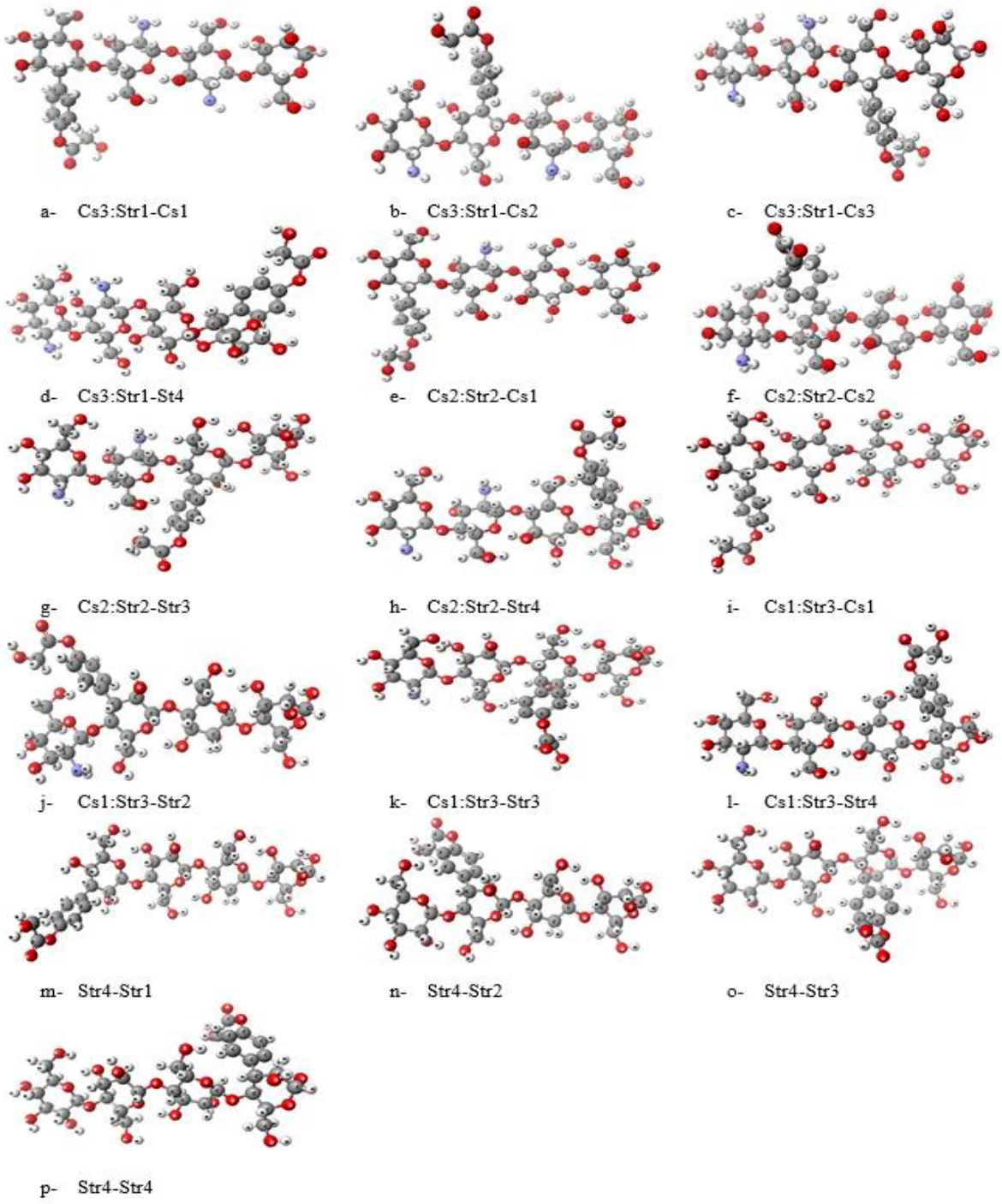

Figure 5. Optimized structures of chitosan/starch ratios with interaction phenol and hydroxymethylcarbonyl for different four units position calculated at PM6 level of theory.

As shown in Tables 1 and 2, the heat of formation decreases with increasing ratio of Cs/Cel and Cs/Str ratios. This means that these compounds with the lowest heat of formation need a small change in enthalpy to form one mole of these compounds. While the heat of formation increases with increasing Cs/Gel ratios. The polarizability values are volume-dependent. The polarizability of Cs/Cel and Cs/Str is slightly the same (Tables 1 and 2), while the polarizability of Cs-Gel compounds decreases with increasing Cs/Gel ratios (table 3).

3.3. Surface area and volume interaction calculation.

The calculated surface area and volume of Cs/Cel, Cs/Str, and Cs/Gel with 3:1, 2:2, and 1:3 ratios modified with phenol and HMC at different four units are shown in the table 4.

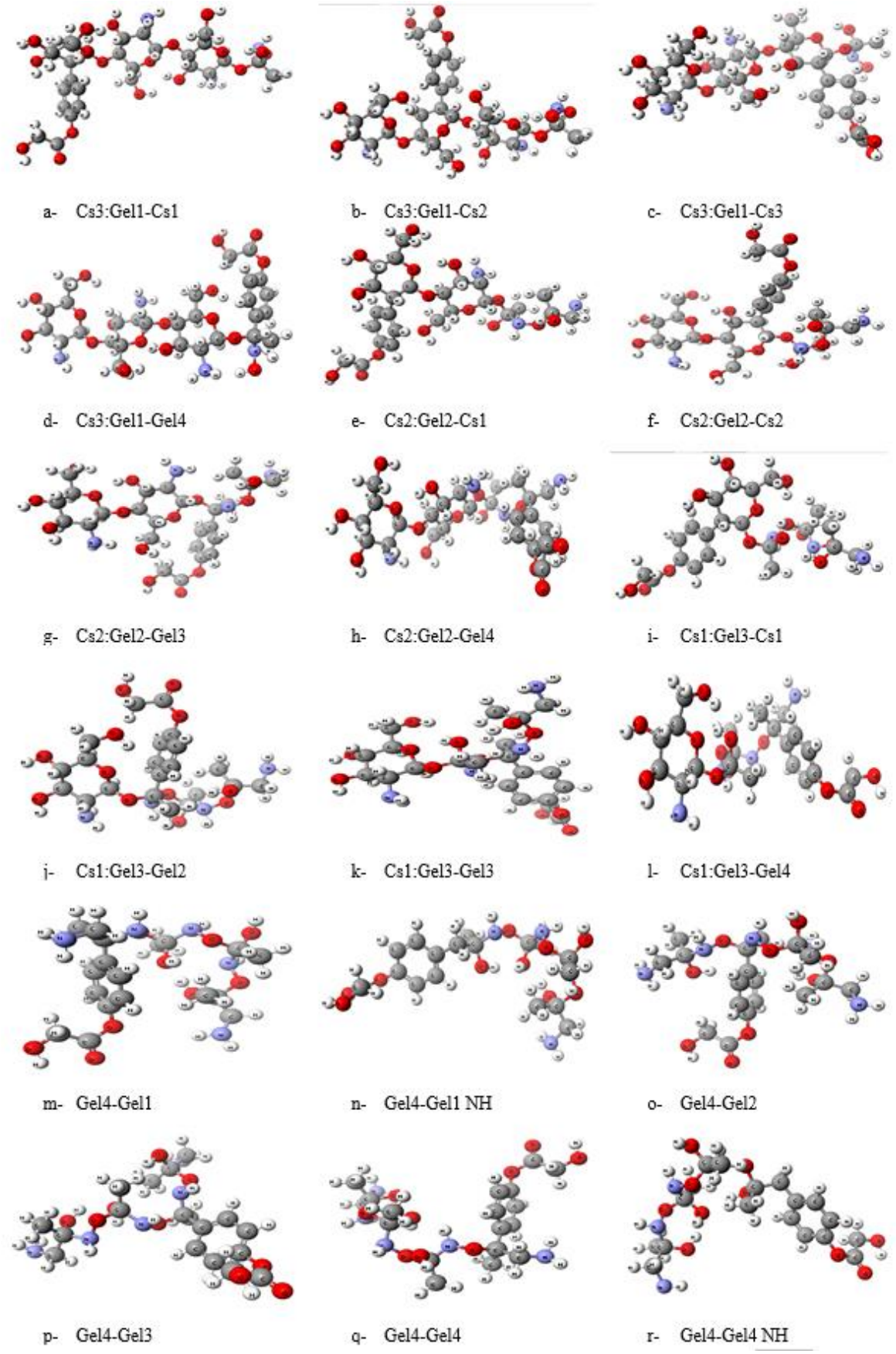

Figure 6. Optimized structures of chitosan/gelatin ratios for interaction with phenol and hydroxymethylcarbonyl at different four units position calculated at PM6 level of theory.

For Cs/Cel ratios, the surface area increases, and volume decrease for the different compounds with increasing Cs/Cel ratios. The surface area and volume are 697.950 A^2 and 601.420 A^3 for Cs3:Cel1-Cel4; 702.590 A^2 and 599.790 A^3 for Cs2:Cel2-Cel4 and 702.590 A^2 and 585.790 A^3 for Cs1:Cel3-Cs1, respectively. For Cs/Str ratios, the surface area and volume increase for 3:1 and 2:2 ratios then decrease again for 1:3 ratio while the surface area and volume of Cs/Gel decrease with increases ratio of Gel to Cs subunits.

From the above data concluded, for Cs/Cel ratios, increasing of Cel to Cs units decrease the solubility of the modified compound while it increases the reactivity of some compounds; especially the compounds modified with phenol and HMC through Cs unit in the Cs/Cel ratios (as Cs1:Cel3-Cs1). For Cs/Str, also increasing of Str to Cs unit decreases solubility while it increases the reactivity of modified compounds interacted through Cs units (as Cs1:Str3-Cs1). More decreasing of solubility by increasing of Gel units in Cs/Gel ratios comparing with Cs/Cel and Cs/Str. The reactivity increase only for modified Gel. All of these compounds will be promising to act as HIV protease inhibitors.

Table 1. Some of the calculated QSAR properties for chitosan/cellulose ratios with the interaction of phenol and HMC for different four units at PM6.

Group %		Structure	log P	Totalenergy [kcal/mol]	Dipole moment [Debye]	ΔE [eV]	Ionization potential [eV]	Polarizability [A^3]	Heat of formation [kcal/mol]
Chitosan : Cellulose	4 : 0	Cs4-Cs1	-5.27	-305449	5.23	9.03	-9.86	53.67	-853.01
		Cs4-Cs2	-5.27	-305450	6.23	9.02	-9.86	53.38	-852.14
		Cs4-Cs3	-5.27	-305446	3.24	9.23	-9.84	53.71	-852.79
		Cs4-Cs4	-5.27	-305455	5.16	9.22	-9.95	52.98	-855.87
	3 : 1	Cs3:Cel1-Cs1	-4.92	-307186	5.69	9.23	-9.75	53.53	-898.05
		Cs3:Cel1-Cs2	-4.92	-307192	4.83	9.19	-9.90	53.04	-899.18
		Cs3:Cel1-Cs3	-4.92	-307175	5.71	9.23	-9.85	53.13	-899.35
		Cs3:Cel1-Cel4	-5.37	-305452	4.87	9.03	-9.87	52.85	-848.14
	2 : 2	Cs2:Cel2-Cs1	-4.58	-308928	7.32	9.25	-9.71	53.47	-941.05
		Cs2:Cel2-Cs2	-4.58	-308942	5.32	9.15	-9.79	52.97	-942.31
		Cs2:Cel2-Cel3	-5.01	-307183	5.42	9.05	-9.93	53.02	-897.49
		Cs2:Cel2-Cel4	-5.01	-307192	1.49	8.98	-9.87	53.77	-894.66
	1 : 3	Cs1:Cel3-Cs1	-4.23	-310667	7.71	9.25	-9.73	53.14	-984.35
		Cs1:Cel3-Cel2	-4.67	-308924	6.36	9.18	-10.05	52.27	-940.69
		Cs1:Cel3-Cel3	-4.67	-308932	3.17	8.95	-9.93	52.82	-936.86
		Cs1:Cel3-Cel4	-4.67	-308934	2.95	8.84	-9.89	53.54	-937.52
	0 : 4	Cel4-Cel1	-4.32	-310664	4.033	9.17	-9.92	52.05	-983.13
		Cel4-Cel2	-4.32	-310669	4.070	9.17	-10.17	51.92	-984.18
		Cel4-Cel3	-4.32	-310672	8.100	9.16	-10.05	52.17	-984.84
		Cel4-Cel4	-4.32	-310672	3.480	9.18	-10.12	52.96	-982.71

Table 2. Some of the calculated QSAR properties for chitosan/starch ratios with the interaction of phenol and HMC at different four units at PM6.

Group			log P	Totalenergy [kcal/mol]	Dipole moment [Debye]	ΔE [eV]	Ionization potential [eV]	Polarizability [A^3]	Heat of formation [kcal/mol]
Chitosan : Starch	4 : 0	Cs4-Cs1	-5.27	-305449	5.23	9.02	-9.86	53.67	-853.01
		Cs4-Cs2	-5.27	-305450	6.23	9.02	-9.86	53.38	-852.14
		Cs4-Cs3	-5.27	-305446	3.24	9.23	-9.84	53.71	-852.79
		Cs4-Cs4	-5.27	-305455	5.16	9.22	-9.95	52.98	-855.87
	3 : 1	Cs3:Str1-Cs1	-4.92	-307190	9.74	8.98	-10.02	52.79	-892.47
		Cs3:Str1-Cs2	-4.92	-307183	6.97	9.21	-9.77	52.37	-895.70
		Cs3:Str1-Cs3	-4.92	-307172	7.71	9.19	-9.87	53.15	-893.67
		Cs3:Str1-St4	-6.45	-259623	5.33	10.15	-10.01	40.97	-797.28
	2 : 2	Cs2:Str2-Cs1	-4.58	-308911	4.28	9.11	-10.09	52.84	-937.69
		Cs2:Str2-Cs2	-4.58	-308911	6.14	9.17	-10.16	52.56	-940.35
		Cs2:Str2-Str3	-5.02	-307174	2.58	9.09	-9.73	52.44	-894.17
		Cs2:Str2-Str4	-5.02	-307181	4.38	9.19	-9.98	51.79	-893.21

Group			log P	Totalenergy [kcal/mol]	Dipole moment [Debye]	ΔE [eV]	Ionization potential [eV]	Polarizability [A^3]	Heat of formation [kcal/mol]
	1 : 3	Cs1:Str3-Cs1	-4.23	-31066	10.15	9.15	-10.29	52.47	-983.33
		Cs1:Str3-Str2	-4.67	-308940	5.58	9.19	-10.02	52.58	-940.33
		Cs1:Str3-Str3	-4.67	-308907	6.05	9.19	-10.03	52.47	-936.11
		Cs1:Str3-Str4	-4.67	-308919	3.31	9.18	-9.89	51.61	-937.77
	0 : 4	Str4-Str1	-4.32	-310673	9.25	9.12	-10.32	53.16	-981.91
		Str4-Str2	-4.32	-310664	5.55	9.13	-10.09	52.49	-981.12
		Str4-Str3	-4.32	-310639	6.41	9.19	-10.04	52.22	-984.08
		Str4-Str4	-4.32	-310671	5.23	9.19	-9.89	52.13	-982.74

Table 3. Some of the calculated QSAR properties for chitosan/gelatin ratios with the interaction of phenol and HMC at different four units at PM6.

Group %		Structure	log P	Totalenergy [kcal/mol]	Dipole moment [Debye]	ΔE [eV]	Ionization potential [eV]	Polarizability [A^3]	Heat of formation [kcal/mol]
Chitosan : Gelatin	4 : 0	Cs4-Cs1	-5.27	-305449	5.23	9.03	-9.86	53.67	-853.01
		Cs4-Cs2	-5.27	-305450	6.23	9.02	-9.86	53.38	-852.14
		Cs4-Cs3	-5.27	-305446	3.24	9.23	-9.84	53.71	-852.79
		Cs4-Cs4	-5.27	-305455	5.16	9.22	-9.95	52.98	-855.87
	3 : 1	Cs3:Gel1-Cs1	-3.06	-273109	2.69	9.19	-9.94	47.28	-741.55
		Cs3:Gel1-Cs2	-3.06	-273104	6.03	9.17	-9.94	46.88	-750.05
		Cs3:Gel1-Cs3	-3.06	-273116	4.68	9.19	-9.86	47.45	-743.41
		Cs3:Gel1-Gel4	-3.70	-271344	5.27	9.12	-9.84	47.56	-688.01
	2 : 2	Cs2:Gel2-Cs1	-3.27	-190196	3.43	10.12	-9.87	29.99	-530.91
		Cs2:Gel2-Cs2	-1.74	-237748	4.88	9.13	-9.85	41.58	-624.94
		Cs2:Gel2-Gel3	-3.27	-190196	3.43	10.12	-9.87	29.99	-530.91
		Cs2:Gel2-Gel4	-2.91	-235978	4.88	9.16	-9.76	41.97	-569.40
	1 : 3	Cs1:Gel3-Cs1	0.23	-205436	1.26	-9.65	-9.65	36.47	-515.59
		Cs1:Gel3-Gel2	-0.42	-203661	5.59	-9.78	-9.78	35.74	-462.51
		Cs1:Gel3-Gel3	-0.42	-203667	3.60	-9.69	-9.69	36.86	-458.49
		Cs1:Gel3-Gel4	-0.95	-203676	6.69	-9.69	-9.69	36.09	-460.62
	0 : 4	Gel4-Gel1	0.39	-174115	4.224	8.99	-9.52	31.24	-306.51
		Gel4-Gel1 NH	1.60	-175855	7.072	9.22	-9.61	32.05	-363.73
		Gel4-Gel2	0.93	-174080	6.157	8.86	-9.53	31.51	-302.69
		Gel4-Gel3	0.93	-174079	3.662	8.62	-9.51	32.89	-302.93
		Gel4-Gel4	0.39	-174082	9.084	8.84	-9.39	32.26	-303.28
		Gel4-Gel4 NH	1.60	-175829	7.379	9.09	-9.59	32.14	-366.38

Table 4. Calculated surface area and volume of chitosan/cellulose, chitosan/starch, and chitosan/gelatin with 3:1, 2:2, and 1:3 rations modified with phenol and HMC at different four units at PM6.

			Surface Area [A^2]	Volume [A^3]			Surface Area [A^2]	Volume [A^3]			Surface Area [A^2]	Volume [A^3]
Chitosan : Cellulose	3 : 1	Cs3:Cel1-Cs1	698.990	596.940	Chitosan : Starch	3 : 1	Cs3:Str1-Cs1	686.600	599.350	Chitosan : Gelatin	Cs3:Gel1-Cs1	623.830	541.950
		Cs3:Cel1-Cs2	692.940	597.230			Cs3:Str1-Cs2	689.350	598.080		Cs3:Gel1-Cs2	607.810	539.290
		Cs3:Cel1-Cs3	676.240	595.480			Cs3:Str1-Cs3	689.350	596.160		Cs3:Gel1-Cs3	622.440	540.500
		Cs3:Cel1-Cel4	697.950	601.420			Cs3:Str1-St4	572.130	499.950		Cs3:Gel1-Gel4	619.190	545.790
	2 : 2	Cs2:Cel2-Cs1	687.870	593.740		2 : 2	Cs2:Str2-Cs1	686.920	591.860		Cs2:Gel2-Cs1	448.940	390.460
		Cs2:Cel2-Cs2	692.490	592.430			Cs2:Str2-Cs2	678.160	591.910		Cs2:Gel2-Cs2	562.290	489.440
		Cs2:Cel2-Cel3	691.380	598.410			Cs2:Str2-Str3	687.010	598.660		Cs2:Gel2-Gel3	448.940	390.460
		Cs2:Cel2-Cel4	702.590	599.790			Cs2:Str2-Str4	690.030	602.090		Cs2:Gel2-Gel4	561.610	496.360
	1 : 3	Cs1:Cel3-Cs1	702.590	585.790		1 : 3	Cs1:Str3-Cs1	680.820	586.800		Cs1:Gel3-Cs1	480.890	425.630
		Cs1:Cel3-Cel2	687.290	590.120			Cs1:Str3-Str2	678.850	590.740		Cs1:Gel3-Gel2	474.340	428.370
		Cs1:Cel3-Cel3	697.470	593.930			Cs1:Str3-Str3	673.970	588.800		Cs1:Gel3-Gel3	491.270	432.100
		Cs1:Cel3-Cel4	683.720	592.980			Cs1:Str3-Str4	676.850	592.400		Cs1:Gel3-Gel4	489.260	432.070

4. Conclusions

The molecular modeling analysis with PM6 and QSAR descriptors indicate that the studied, modified polymers blends show a change in their physical properties. The results indicate that the modified blends could be intact with amino acids as promising to act as HIV protease inhibitors according to the unique surface properties, hydrogen bonding, and excellent physical properties. The solubility of modified blends is decreased by decreasing the Cs units. Based on a total dipole moment, Cs/Cel blend with 1:3 (7.71 Debye) is reactive in comparison with other studied ratios. While Cs/Str blend with 1:3 ratio (10.15 Debye) is the most reactive. Finally, a highly decreasing of solubility by increasing of Gel units in Cs/Gel ratios comparing with Cs/ Cel and Cs/ Str ratios. The reactivity increase only for modified gelatin. The surface area of modified Cs/Cel ratios increases comparing with modified Cs/Str and Cs/Gel ratios. All of these compounds will be promising to act as HIV protease inhibitors.

The present computational work indicated that molecular modeling continues to be an important tool for investigating biomaterials as well as many other systems, which is in good agreement with the previous findings [47-50].

Funding

This research was funded by the Science and Technology Development Fund (STDF), Egypt, Grant No 14990.

Acknowledgments

This research has no acknowledgment.

Conflicts of Interest

The authors declare no conflict of interest.

References

1. Barakat, N.A.M.; Taha, A.; Motlak, M.; Nassar, M.M.; Mahmoud, M.S.; AlDeyab, S.S.; ElNewehy, M.; Kim, H.Y. ZnO&Fe2O3-incoportaed TiO2 nanofibers as super effective photocatalyst for water splitting under visible light radiation. *Appl. Catal., A* **2014**, *481*, 19-26, https://doi.org/10.1016/j.apcata.2014.04.045.
2. Barakat, N.A.M.; Ahmed, E.; Abdelkareem, M.A.; Farghali, A.A.; Nassar, M.M.; El-Newehy, M.H.; Al-Deyab S.S. Ag, Zn and Cd-doped titanium oxide nanofibers as effective photocatalysts for hydrogen extraction from ammonium phosphates. *J. Mol. Catal. A Chem.* **2015**, *409*, 117-126, https://doi.org/10.1016/j.molcata.2015.08.015.
3. Ghouri, Z.K.; Al-Meer, S.; Barakat, N.A.M.; Kim, H.Y. ZnO@C (core@shell) microspheres derived from spent coffee grounds as applicable non-precious electrode material for DMFCs. *Sci. Rep.* **2017**, *7*, https://doi.org/10.1038/s41598-017-01463-3.
4. Sheikh, F.A.; Ju, H.W.; Lee, J.M.; Moon, B.M.; Park, H.J.; Lee, O.J.; Kim, J.H.; Kim, D.K.; Park, C.H. 3D electrospun silk fibroin nanofibers for fabrication of artificial skin *Nanomed. Nanotechnol. Biol. Med.* **2015**, *11*, 681-691, https://doi.org/10.1016/j.nano.2014.11.007.
5. Sheikh, F.A.; Beigh, M.A.; Qadir, A.S.; Qureshi, S.H.; Kim, H. Hydrophilically modified poly(vinylidene fluoride) nanofibers incorporating cellulose acetate fabricated by colloidal electrospinning for future tissue-regeneration applications Polymer Composites. *Polym. Compos.* **2019**, *40*, 1619-1630, https://doi.org/10.1002/pc.24910.
6. Wu, X.M.; Branford-White, C.J.; Zhu, L.M.; Chatterton, N.P.; Yu, D.G. Ester prodrug-loaded electrospun cellulose acetate fiber mats as transdermal drug delivery systems. *J. Mater. Sci. Mater. Med.* **2010**, *21*, 2403-2411, https://doi.org/10.1007/s10856-010-4100-y.
7. Brown, E.E.; Laborie, M.P.G.; Zhang, J. Glutaraldehyde treatment of bacterial cellulose/fibrin composites: impact on morphology, tensile and viscoelastic properties. *Cellulose* **2012**, *19*, 127-137, https://doi.org/10.1007/s10570-011-9617-9.

8. Negrea, P.; Caunii, A.; Sarac, I.; Butnariu, M. The study of infrared spectrum of chitin and chitosan extract as potential sources of biomass. *Dig. J. Nanomat.&Biostruc. (DJNB)* **2015**, *10*, 1129-1138.
9. Kozakevych, R.; Bolbukh, Y., Tertykh, V. Controlled release of diclofenac sodium from silica-chitosan composites. *World J. Nanosci. Eng.* **2013**, *3*, 69-78, http://dx.doi.org/10.4236/wjnse.2013.33010.
10. Mahatmanti, F.W.; Nuryono, N.; Narsito, N. Physical Characteristics of Chitosan Based Film Modified With Silica and Polyethylene Glycol. *Indones. J. Chem*. **2014,** *14*, 131-137, doi: https://doi.org/10.22146/ijc.21249
11. Gajendiran, M.; Choi, J.; Kim, S.J.; Kim, K.; Shin, H.; Koo, H.J.; Kim, K. Conductive biomaterials for tissue engineering applications. *J. Ind. Eng. Chem.* **2017**, *51*, 12-26, https://doi.org/10.1016/j.jiec.2017.02.031.
12. Kitsara, M.; Agbulut, O.; Kontziampasis, D.; Chen, Y.; Menasché, P. Fibers for hearts: A critical review on electrospinning for cardiac tissue engineering. *Acta Biomater*. **2017,** *48*, 20-40, https://doi.org/10.1016/j.actbio.2016.11.014.
13. Tsai, I.L.; Hsu, C.C.; Hung, K.H.; Chang, C.W.; Cheng, Y.H. Applications of biomaterials in corneal wound healing. *J. Chin. Med. Assoc.* **2015,** *78*, 212-217, https://doi.org/10.1016/j.jcma.2014.09.011.
14. Singh, D.G.; Kaur, S.; Jyoti, S.S.; Kaur, B.S.; Verma, M.; Yadagiri, S.R. Recent development in applications of important biopolymer chitosan in biomedicine, pharmaceuticals and personal care products. *Current Tissue Eng*. **2013,** *2*, 20-40, https://doi.org/10.2174/2211542011302010004.
15. Latif, U.; Al-Rubeaan, K.; Saeb, A.T. A review on antimicrobial chitosan-silver nanocomposites: a roadmap toward pathogen targeted synthesis. *Int J Polymer Mater Polymer Biomater*. **2015,** *64*, 448-458, https://doi.org/10.1080/00914037.2014.958834.
16. Morsi, R.E.; Alsabagh, A.M.; Nasr, S.A.; Zaki, M.M. Multifunctional nanocomposites of chitosan, silver nanoparticles, copper nanoparticles and carbon nanotubes for water treatment: antimicrobial characteristics. *Int. J. BiolMacromol*. **2017**, *97*, 264-269, https://doi.org/10.1016/j.ijbiomac.2017.01.032.
17. Rizzo, L.Y.; Golombek, S.K.; Mertens, M.E.; Pan, Y.; Laaf, D.; Broda, J.; Jayapaul, J.; Möckel, D.; Subr, V.; Hennink, W. E.; Storm, G.; Simon, U.; Jahnen-Dechent, W.; Kiessling, F.; Lammers, T. In vivo nanotoxicity testing using the zebrafish embryo assay. *J Mater Chem B*. **2013,** *1*, 3918-3925, https://doi.org/10.1039/C3TB20528B.
18. Asghari, S.; Johari, S.A.; Lee, J.H.; Kim, Y.S.; Jeon, Y.B.; Choi, H.J.; Moon, M.C.; Yu, I. J. Toxicity of various silver nanoparticles compared to silver ions in Daphnia magna. *J Nanobiotechnology* **2012,** *10*, https://doi.org/10.1186/1477-3155-10-14.
19. Abu-Elala, N.M.; AbuBakr, H.O.; Khattab, M.S.; Mohamed, S.H.; El-Hady, M.A.; Ghandour, R.A.; Morsi, R.E. Aquatic environmental risk assessment of chitosan/silver, copper and carbon nanotube nanocomposites as antimicrobial agents. *Int J Biol Macromol*. **2018**, *113*, 1105-1115, https://doi.org/10.1016/j.ijbiomac.2018.03.047.
20. Khakpour, R.; Tahermansouri, H. Synthesis, characterization and study of sorption parameters of multi-walled carbon nanotubes/chitosan nanocomposite for the removal of picric acid from aqueous solutions. *Int J Biol Macromol*. **2018,** *109*, 598-610, https://doi.org/10.1016/j.ijbiomac.2017.12.105.
21. Ahmed, M.A.; Abdelbar, N.M.; Mohamed, A.A. Molecular imprinted chitosan-TiO_2 nanocomposite for the selective removal of rose bengal from wastewater. *Int J Biol Macromol*. **2018,** *107*, 1046-1053, https://doi.org/10.1016/j.ijbiomac.2017.09.082.
22. Erdem, B.; Erdem, M.; Özcan, A.S. Adsorption of Reactive Black 5 onto quaternized 2-dimethylaminoethyl methacrylate based polymer/clay nanocomposites. *Adsorpt*. **2016,** *22*, 767-776, https://doi.org/10.1007/s10450-016-9773-1.
23. Thomas, M.; Naikoo, G.A.; Sheikh, M.U.D.; Bano, M.; Khan, F. Effective photocatalytic degradation of Congo red dye using alginate/carboxymethyl cellulose/TiO_2 nanocomposite hydrogel under direct sunlight irradiation. *J Photochem Photobiol A: Chem*. **2016,** *327*, 33-43, https://doi.org/10.1016/j.jphotochem.2016.05.005.
24. Sarkar, A.K.; Saha, A.; Tarafder, A.; Panda, A.B.; Pal, S. Efficient removal of toxic dyes via simultaneous adsorption and solar light driven photodegradation using recyclable functionalized amylopectin–TiO2–Au nanocomposite. *ACS Sustain Chem Eng*. **2016,** *4*, 1679-1688, https://doi.org/10.1021/acssuschemeng.5b01614.
25. Pathania, D.; Katwal, R.; Sharma, G.; Naushad, M.; Khan, M.R.; Ala'a, H. Novel guar gum/Al2O3 nanocomposite as an effective photocatalyst for the degradation of malachite green dye. *Int J Biol Macromol*. **2016,** *87*, 366-374, https://doi.org/10.1016/j.ijbiomac.2016.02.073.
26. Gulzar, A.; Yang, P.; He, F.; Xu, J.; Yang, D.; Xu, L.; Jan, M.O. Bioapplications of graphene constructed functional nanomaterials. *Chem Biol Interact*. **2017,** *262*, 69-89, https://doi.org/10.1016/j.cbi.2016.11.019.
27. Bhawani, S.A.; Bhat, A.H.; Ahmad, F.B.; Ibrahim, M.N.M. Green polymer nanocomposites and their environmental applications. *Woodhead Publishing Series in Composites Science and Engineering* **2018,** 617-633, https://doi.org/10.1016/B978-0-08-102262-7.00023-4.
28. Xu, R.; Mao, J.; Peng, N.; Luo, X.; Chang, C. Chitin/clay microspheres with hierarchical architecture for highly efficient removal of organic dyes. *Carbohydr polym*. **2018,** *188*, 143-50, https://doi.org/10.1016/j.carbpol.2018.01.073.

29. Gouthaman, A.; Azarudeen, R.S.; Gnanaprakasam, A.; Sivakumar, V.; Thirumarimurugan, M. Polymeric nanocomposites for the removal of Acid red 52 dye from aqueous solutions: Synthesis, characterization, kinetic and isotherm studies. *Ecotoxicol Environ Saf.* **2018,** *160*, 42-5, https://doi.org/10.1016/j.ecoenv.2018.05.011.
30. Hansch, C.; Leo, A. *Exploring QSAR: Fundamentals and Applications in Chemistry and Biology.* American Chemical Society. Washington, DC. **1995.**
31. Cohen, N.C. *Guidebook on Molecular Modeling in Drug Design.* First ed., Academic press, Inc. **1996**; https://doi.org/10.1016/B978-0-12-178245-0.X5000-8.
32. Atkin, P.W.; de Paula, *J. Physical Chemistry*. Freeman, W.H. NY. Sections 21, **2002**; pp. 2-4.
33. Garg, R.; Bhhatarai, B. QSAR and Molecular Modeling Studies of HIV Protease Inhibitors. *Top Heterocycl Chem.* **2006,** *3*, 181-271, https://doi.org/10.1007/7081_038.
34. Gupta, S.P. *QSAR and Molecular Modeling, Springer Basel/Anamaya*. New Delhi. **2011.**
35. Bissantz, C.; Kuhn, B.; Stahl, M. A medicinal chemist's guide to molecular interactions. *J. Med. Chem*. **2010,** *53*, 5061-5084, https://doi.org/10.1021/jm100112j.
36. Jin, X.; Peldszus, S.; Huck, P.M. Predicting the reaction rate constants of micropollutants with hydroxyl radicals in water using QSPR modeling. *Chemosphere* **2015,** *138*, 1-9, https://doi.org/10.1016/j.chemosphere.2015.05.034.
37. Thareja, S. Steroidal 5alpha-Reductase Inhibitors: A Comparative 3D-QSAR Study Review. *Chem. Rev.* **2015,** *115*, 2883-2894, https://doi.org/10.1021/cr5005953.
38. Yu, S.; Zhou, Q.; Zhang, X.; Jia, S.; Gan, Y.; Zhang, Y.; Shi, J.; Yuan, J. Hologram quantitative structure–activity relationship and topomer comparative molecular-field analysis to predict the affinities of azo dyes for cellulose fibers. *Dyes Pigments* **2018,** *153*, 35-43, https://doi.org/10.1016/j.dyepig.2018.01.053.
39. Turkmenoğlu, B.; Yilmaz, H.; Su, E. M.; Alp Tokat, T.; Guzel, Y. 4D-QSAR study of flavonoid derivatives with MCET method. *Int. J. Chem. Technol.* **2017,** *1*, 14–23, https://doi.org/10.32571/ijct.338920.
40. Türkmenoğlu, B.; Güzel, Y. Molecular docking and 4D-QSAR studies of metastatic cancer inhibitor thiazoles. *Comput Biol Chem*. **2018,** *76*, 327–337, https://doi.org/10.1016/j.compbiolchem.2018.07.003.
41. Villaverde, J.J.; Sevilla-Morán, B.; López-Goti, C.; Alonso-Prados, J.L.; Sandín-España, P. Computational methodologies for the risk assessment of pesticides in the European Union. *J. Agric. Food Chem.* **2017,** *65*, 2017-2018, https://doi.org/10.1021/acs.jafc.7b00516.
42. Stewart, J.J.P.; Version MO-G 1.1A. *Fujitsu Limited, Tokyo*. Japan, **2008**.
43. Al-Fifi, Z.; Saleh, N.A.; Elhaes, H.; Ibrahim, M. On the Molecular Modeling Analyses of Novel HIV-1 Protease Inhibitors Based on Modified Chitosan Dimer. *Int. J. Spectrosc.* **2015,** *2015*, 1-9, https://doi.org/10.1155/2015/174098.
44. Ibrahim, M.; El-Haes, H. Computational spectroscopic study of copper, cadmium, lead and zinc interactions in the environment. *Int. J. Environ. Pollut.* **2005,** *23*, 417–424, https://doi.org/10.1504/IJEP.2005.007604.
45. Ibrahim, M.; Saleh, N.A.; Elshemey W.M. In Quantitative Structure Activity Relationship. In: *Recent Trends on QSAR in the Pharmaceutical Perceptions.* Edited Khan, M.T.H. Bentham Science Publishers **2012;** pp. 360-391.
46. Lakhanpal, M.L. *Fundamentals of Chemical Thermodynamics*. Tata McGraw-Hill Publishing Company Limited **1983**.
47. Afzal, M.A.F.; Hachmann, J. Benchmarking DFT approaches for the calculation of polarizability inputs for refractive index predictions in organic polymers. *Phys. Chem. Chem. Phys.* **2019**, *21*, 4452-4460, https://doi.org/10.1039/C8CP05492D.
48. Ponzoni, I.; Sebastián-Pérez, V.; Martínez, M.J.; Roca, C.; Pérez, C.C.; Cravero, F.; Vazquez, G.E.; Páez, J.A.; Díaz, M.F.; Campillo, N.E. QSAR Classification Models for Predicting the Activity of Inhibitors of Beta-Secretase (BACE1) Associated with Alzheimer's disease. *Sci Rep* **2019**, *9*, https://doi.org/10.1038/s41598-019-45522-3.
49. Fahim, A.M.; Shalaby M.A.; Ibrahim, M. Microwave-assisted synthesis of novel 5-aminouracil-based compound with DFT calculations. *J. Mol. Struct.* **2019**, *1194*, 211-226, https://doi.org/10.1016/j.molstruc.2019.04.078.
50. El-Mansy. M.A.M.; Osman, O.; Mahmoud, A.A.; Elhaes, H.; Ibrahim, M. Computational Notes on the Molecular Modeling Analyses of Flutamide. *Letters in Applied NanoBioScience* **2020**, *9*, 1099-1102, https://doi.org/10.33263/LIANBS92.10991102.